ACTA IMEKO
ISSN: 2221-870X
September 2023, Volume 12, Number 3, 1 - 9

A solar PV model parameters estimation based on an improved manta foraging algorithm with dynamic fitness distance balance

Mouncef El Marghichi[1], Soufiane Dangoury[2], Mohammed Amine Amlila[3]

[1] *Faculty of Sciences and Technology, Hassan first University, FST of Settat, Km 3, B.P: 577 Road to Casablanca, Settat, Morocco*
[2] *Hassan II University of, Casablanca, Morocco*
[3] *Laboratory of Engineering Sciences for Energy (LabSIPE) ENSA, University Chouaib Doukkali, El Jadida, Morocco*

ABSTRACT
Accurately simulating and operating photovoltaic (PV) modules or solar cells requires determining specific model parameters based on experimental data. Extracting these parameters is crucial for analyzing system performance under various conditions such as temperature and sunlight variations. However, modeling solar photovoltaic systems is inherently nonlinear, which calls for an efficient algorithm. In this study, we employ the MRFO-dFDB (Manta Ray Foraging Optimization with dynamic Fitness Distance Balance) algorithm, which utilizes fitness distance balance to balance the exploration and exploitation of the search area when assessing parameters in solar PV models. By applying MRFO-dFDB to extract parameters from the STP6-120/36 and Photowatt-PWP201 solar modules, we observe exceptional predictive performance for both single diode (SDM) and double diode (DDM) models. MRFO-dFDB exhibits superior performance compared to state-of-the-art methods. It achieves lower Root-Mean-Square Error (RMSE) values, specifically < 15.3 mA for the STP6-120/36 module and <2.4 mA for the Photowatt-PWP201 module. Additionally, it demonstrates lower maximum errors of 39.02 mA and 5.33 mA, as well as lower power errors of 155.42 mW and 14.122 mW, for the STP6-120/36 and Photowatt-PWP201 solar modules, respectively. Furthermore, it exhibits excellent performance with faster computation speed (< 30.1 seconds in all tests), further emphasizing its superiority.

Section: RESEARCH PAPER

Keywords: Manta ray foraging optimization with Dynamic fitness distance balance (MRFO-dFDB); PV parameter extraction; PV model; solar PV

Citation: Mouncef El Marghichi, Soufiane Dangoury, Mohammed Amine Amlila, A solar PV model parameters estimation based on an improved manta foraging algorithm with dynamic fitness distance balance, Acta IMEKO, vol. 12, no. 3, article 55, September 2023, identifier: IMEKO-ACTA-12 (2023)-03-55

Section Editor: Francesco Lamonaca, University of Calabria, Italy

Received April 29, 2023; **In final form** August 1, 2023; **Published** September 2023

Corresponding author: Mouncef El marghichi, e-mails: Elmarghichi.mouncef@gmail.com; m.elmarghichi@uhp.ac.ma

1. INTRODUCTION

The increasing prevalence of renewable energy sources can be attributed to various factors related to climate change, energy needs, and energy scarcity. Photovoltaic power plants, which rely on solar power systems, play a crucial role in generating electricity on a large scale. However, these systems are often installed in open areas, making them susceptible to damage from severe weather conditions like rainstorms and gales. To address this challenge, the development of an accurate data-driven model is essential for determining the key characteristics of photovoltaic systems used in the solar industry. Analysing solar model parameters provides numerous benefits, including evaluating the performance of photovoltaic power plants, computing energy efficiency, implementing maximum power point tracking (MPPT), and optimizing the system's energy management [1].

To model solar photovoltaic systems effectively, two stages are required: the development of a mathematical model and identification of its parameters. Among the models available, the single-diode model (SDM) and double-diode model (DDM) are widely utilized [2]. However, the performance of these models can lose its stability and unreliable due to unspecified parameters, particularly if the equipment undergoes contingent aging. Therefore, accurate parameter estimation is an important task when working with photovoltaic cell models [3]. In addition, the optimization and installation of photovoltaic systems require precise modelling. Nevertheless, the PV model is non-linear and has a non-convex relationship, which poses several challenges

and obstacles. Efforts have been made by researchers to find ways of accurately assessing the unknown parameters. These efforts have resulted in the identification of three methods: analytical, deterministic, and metaheuristic techniques [4].

The utilization of analytical methods involves the utilization of particular data points, such as the short-circuit point, open-circuit point, and maximum power point found on the current-voltage (I-V) characteristic curve under standard test conditions (STC). These methods are characterized by their simplicity, speed, and convenience, and are utilized to develop a handful of equations to handle the unknown parameters of the model. However, the accuracy of these methods is heavily reliant on the accuracy of the selected data points given by the manufacturers. If these values are incorrectly specified, it will significantly degrade the extraction accuracy due to the "taking a part for the whole" extraction strategy. Furthermore, the special data points utilized in these methods are factory measured under STC conditions, but as time passes, the model parameters may change due to PV degradation, further affecting the accuracy of the "taking a part for the whole" methods [5]-[6].

Deterministic techniques employ the "take all measured data for the entire system" strategy to extract unknown parameters. Accurately extracting these parameters requires a considerable amount of measurements [7]. These techniques rely on a loss function that measures the distinction between the predicted and measured data points. Due to their utilization of gradient information, deterministic methods may converge to a local optimal solution.

Algorithms that rely on evolutionary principles, such as the evolutionary strategy algorithm (ESA) [8], differential evolutionary algorithm (DEA) [9], and genetic algorithm (GA) [10] are known as evolutionary-based algorithms.

In contrast to deterministic methods, metaheuristic approaches do not rely on gradient information and avoid simplification or linearization during optimization. As a result, they have gained increasing attention as an alternative to deterministic methods. Various metaheuristic techniques, such as particle swarm optimization (PSO) [11], teaching-learning-based optimization (TLBO) [12], artificial bee colony (ABC) [13], JAYA algorithm [14], supply-demand-based optimization (SDO) [15], symbiotic organisms search algorithm (SOS) [16], imperialist competitive algorithm [17], flower pollination algorithm (FPA) [18], and hybrid algorithms [19]-[21], have been used to extract parameters from PV models.

When it comes to modelling PV modules and cells, analogue electrical circuits are the preferred method for achieving accuracy. Photovoltaic researchers commonly utilize SDM and DDM modelling approaches. Simulation of single-diode cells and modules requires five parameters, while double-diode cells and modules require seven. Precise estimation of these parameters with an absolute minimum error between the calculated and measured currents is crucial to achieving precise simulation of the I-V physical system features.

Existing literature has identified research gaps in the areas solar cell parameters identification and metaheuristic optimization. These shortcomings involve the use of non-adaptive weight metrics in the metaheuristic approaches, the calculation speed, the risk of metaheuristic algorithms becoming trapped in local best optima, and the necessity to further minimize RMSE (root mean square error) values produced by most algorithms.

To address the limitations in solar cell parameter identification, it is necessary to bridge the research gap. This paper introduces a new metaheuristic algorithm, named MRFO-DFDB (Manta Ray Foraging Optimization with Dynamic Fitness Distance Balance). The algorithm utilizes fitness distance balance to balance both exploration and exploitation of the search space when estimating parameters in solar PV models. The fitness distance balance measure assesses population diversity and adjusts the exploration and exploitation parameters accordingly. The dynamic nature of the fitness distance balance enables the algorithm to adapt to changes in the search space and maintain an optimal balance between exploration and exploitation. This enables the algorithm to find the optimal solar PV parameters rapidly with good efficiency.

Our algorithm demonstrates superior performance by achieving the lowest fitness value with minimal iterations compared to the WOS (War Strategy Optimization Algorithm) and the SFO (Sunflower Optimization Algorithm), showcasing its efficiency and speed. We conducted tests on two different modules, namely STP6-120/36 and Photowatt-PWP201, and compared the results to those obtained using the SFO and WOS algorithms. Our results validate the algorithm's robustness, speed, and efficiency, making it a suitable choice for estimating parameters for solar PV models.

This document is structured as follows: In Section 2, we introduce the solar PV models used in our research, including the relevant equations. Section 3 provides an overview of the algorithm implementation steps. The implementation setup for the STP6-120/36 and Photowatt-PWP201 tests are reported un Section 4, the discussion of results is presented in Section 5. Finally, in Section 6, we draw the conclusion.

2. SOLAR PV MODELLING

This section covers the mathematical models related to solar PV cells and modules.

2.1. Single-Diode Model (SDM)

There are various equivalent circuits that can represent the I-V characteristics of PV modules, the most commonly used and renowned for its simplicity and accuracy is the Single-Diode Model (SDM) as depicted in Figure 1 [22]. This model utilizes a single-diode approximation to relate the different variables, and it includes several parameters such as I_{out} (output current), I_{sh} (shunt resistance current), R_s (series resistance), I_{ph} (photocurrent), I_o (diode current), and R_{sh} (shunt resistance) as depicted below:

The current I_o and I_{sh} are expressed by:

$$I_o = I_{sd}\left(e^{\frac{q\,(I_{out}R_s+V)}{n\,K\,T}} - 1\right), \tag{1}$$

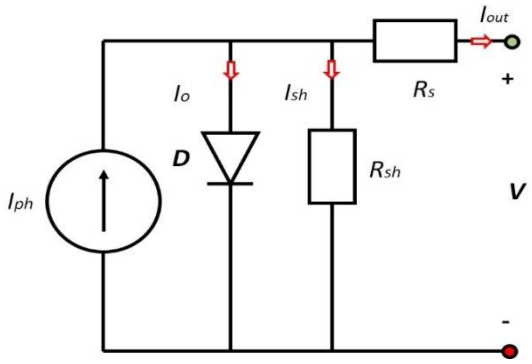

Figure 1. SDM equivalent circuit.

$$I_{\mathrm{sh}} = \frac{I_{\mathrm{out}}\, R_{\mathrm{s}} + V}{R_{\mathrm{sh}}}, \tag{2}$$

with I_{out} expressed as:

$$I_{\mathrm{out}} = I_{\mathrm{ph}} - I_{\mathrm{sh}} - I_{\mathrm{o}}\,. \tag{3}$$

The output current of the PV is outlined by the following formula:

$$I_{\mathrm{out}} = I_{\mathrm{ph}} - I_{\mathrm{sd}}\left(\mathrm{e}^{\frac{q(I_{\mathrm{out}} R_{\mathrm{s}}+V)}{n\,K\,T}} - 1\right) - \frac{I_{\mathrm{out}}\, R_{\mathrm{s}} + V}{R_{\mathrm{sh}}}. \tag{4}$$

In accordance with [23], the symbol I_{sd} denotes the saturation current of the reverse diode, while q represents the elementary charge of an electron (1.602×10^{-19} C). Additionally, K denotes the Boltzmann constant, V signifies the voltage output of the cell, R_{s} stands for the resistance in series, n represents the diode ideality factor, T denotes the temperature in Kelvin, and R_{sh} is the resistance in shunt.

2.2. Double-Diode Model (DDM)

The DDM circuit, depicted in Figure 2, is an alternative circuit model utilized to tackle the energy loss problem that is not accounted for by the SDM. The current I_{out} in the DDM circuit can be calculated using the following formula:

$$I_{\mathrm{out}} = I_{\mathrm{ph}} - I_{\mathrm{o1}} - I_{\mathrm{o2}} - I_{\mathrm{sh}}\,. \tag{5}$$

The symbols I_{o2} and I_{o1} are used to denote the currents flowing through the second and first diodes, respectively.

$$I_{\mathrm{o1}} = I_{\mathrm{sd1}}\left(\mathrm{e}^{\frac{q\,(V+I_{\mathrm{out}} R_{\mathrm{s}})}{n_1\,K\,T}} - 1\right), \tag{6}$$

$$I_{\mathrm{o2}} = I_{\mathrm{sd2}}\left(\mathrm{e}^{\frac{q\,(V+I_{\mathrm{out}} R_{\mathrm{s}})}{n_2\,K\,T}} - 1\right). \tag{7}$$

The current I_{out} can be determined by applying Equation (8), where the ideality factor of the diodes is represented by n_2 and n_1

$$\begin{aligned} I_{\mathrm{out}} &= I_{\mathrm{ph}} - I_{\mathrm{sd1}}\left(\mathrm{e}^{\frac{q\,(I_{\mathrm{out}} R_{\mathrm{s}}+V)}{n_1\,K\,T}} - 1\right) \\ &\quad - I_{\mathrm{sd2}}\left(\mathrm{e}^{\frac{q\,(I_{\mathrm{out}} R_{\mathrm{s}}+V)}{n_2\,K\,T}} - 1\right) - \frac{I_{\mathrm{out}}\, R_{\mathrm{s}} + V}{R_{\mathrm{sh}}}. \end{aligned} \tag{8}$$

2.3. PV Module Model

The output current I_{out} of a photovoltaic (PV) module comprising $N_{\mathrm{p}} \times N_{\mathrm{s}}$ solar cells arranged in parallel and/or series can be expressed as follows:

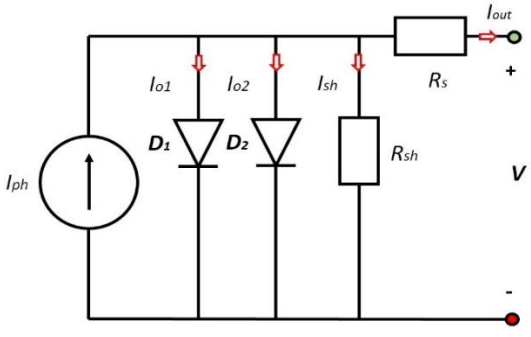

Figure 2. DDM equivalent circuit.

- when considering the SDM based PV module:

$$\begin{aligned} I_{\mathrm{out}} &= I_{\mathrm{ph}} - I_{\mathrm{sd}}\left(\mathrm{e}^{\frac{q\left(V/N_{\mathrm{s}}+I\,R_s/N_{\mathrm{p}}\right)}{n\,K\,T}} - 1\right) \\ &\quad - \frac{I_{\mathrm{out}}\, R_{\mathrm{s}}/N_{\mathrm{p}} + \mathrm{V}/N_{\mathrm{s}}}{R_{\mathrm{sh}}}, \end{aligned} \tag{9}$$

- for the DDM:

$$\begin{aligned} I_{\mathrm{out}} &= I_{\mathrm{ph}} - I_{\mathrm{sd1}}\left(\mathrm{e}^{\frac{q\left(I_{\mathrm{out}} R_{\mathrm{s}}/N_{\mathrm{p}}+V/N_{\mathrm{s}}\right)}{n_1\,K\,T}} - 1\right) \\ &\quad - I_{\mathrm{sd2}}\left(\mathrm{e}^{\frac{q\left(V/N_{\mathrm{s}}+I_{\mathrm{out}} R_{\mathrm{s}}/N_{\mathrm{p}}\right)}{n_2\,K\,T}} - 1\right) \\ &\quad - \frac{I_{\mathrm{out}}\, R_{\mathrm{s}}/N_{\mathrm{p}} + \mathrm{V}/N_{\mathrm{s}}}{R_{sh}}. \end{aligned} \tag{10}$$

2.4. Objective function

The primary objective of this study is to reduce the difference between the current simulated by the model and the current measured from the solar cell. To achieve this, a popular and accurate approach is to utilize the root mean square error (RMSE) as a loss function, which allows for the identification of optimal parameter values for the PV model. In this research, the Dynamic FDB selection method is utilized to extract the parameters of a solar PV system through voltage and current measurements. The loss function is formulated based on the deviation between the measured I_{meas} and the estimated I_{estim} current, which is quantified as follows:

$$F_{\mathrm{loss}} = \sqrt{\frac{1}{N}\left(\sum_{i=1}^{N} |I_{\mathrm{estim}} - I_{\mathrm{meas}}|^2\right)}. \tag{11}$$

3. MRFO-DFDB ALGORITHM

3.1. MRFO

The Manta Ray Foraging Optimization (MRFO) algorithm is a metaheuristic optimization algorithm that is inspired by the foraging behaviours of manta rays in the ocean. The algorithm uses a population-based approach to iteratively search for optimal solutions to a given problem [24].

The foraging behaviours of manta rays, namely chain foraging, cyclone foraging, and somersault foraging, are modelled mathematically to guide the search process. Below are the descriptions of the corresponding mathematical models.

3.1.1. Chain foraging

MRFO uses manta rays that locate and swim towards positions with higher concentrations of plankton, assuming those positions contain the best solution. Manta rays form a foraging chain and move towards both the food and the individual in front of them. This mathematical model is described as:

$$\begin{aligned} x_i^d(t+1) &= \begin{cases} x_i^d(t) + r\cdot\left(x_{\mathrm{best}}^d(t) - x_i^d(t)\right) + \alpha\cdot\left(x_{\mathrm{best}}^d(t) - x_i^d(t)\right), i = 1 \\ x_i^d(t) + r\cdot\left(x_{i-1}^d(t) - x_i^d(t)\right) + \alpha\cdot\left(x_{\mathrm{best}}^d(t) - x_i^d(t)\right), i = 2\,..\,N \end{cases}, \end{aligned} \tag{12}$$

$$\alpha = 2\cdot r\cdot\sqrt{|\log(r)|}\,. \tag{13}$$

The position of the *i*-th individual in the *d*-th dimension at time *t* is represented by $x_i^d(t)$. The update of the *i*-th individual's position is determined by the (*i*-1)th individual's position $x_{i-1}(t)$, and the position of the food with high concentration $x_{\text{best}}^d(t)$. This update is computed using a weight coefficient α, and a random vector *r* within the range of [0, 1].

3.1.2. Cyclone foraging

Manta rays form a foraging chain and swim towards patches of plankton by spiralling when they are in deep water. In the cyclone foraging strategy, each manta ray not only spirals towards the food, but also swims towards the individual in front of it, forming a line that spirals. The equation describing this movement of the manta rays in a two-dimensional space can be written as:

$$\begin{Bmatrix} X_i(t+1) = X_{\text{best}} + r.\left(X_{i-1}(t) - X_i(t)\right) + e^{b\omega}.\cos(2\pi\omega).\left(X_{\text{best}}(t) - X_i(t)\right) \\ Y_i(t+1) = Y_{\text{best}} + r.\left(Y_{i-1}(t) - Y_i(t)\right) + e^{b\omega}.\sin(2\pi\omega).\left(Y_{\text{best}}(t) - Y_i(t)\right) \end{Bmatrix} \quad (14)$$

The range of the random number ω is between 0 and 1.

This motion behaviour can be extended to an *n*-dimensional space. For simplicity, the equation describing of cyclone foraging is descried as:

$$x_i^d(t+1) = \begin{Bmatrix} x_{\text{best}}^d + r \cdot \left(x_{\text{best}}^d(t) - x_i^d(t)\right) + \beta \cdot \left(x_{\text{best}}^d(t) - x_i^d(t)\right), i = 1 \\ x_{\text{best}}^d + r \cdot \left(x_{i-1}^d(t) - x_i^d(t)\right) + \beta \cdot \left(x_{\text{best}}^d(t) - x_i^d(t)\right), i = 2..N \end{Bmatrix} \quad (15)$$

$$\beta = 2 \cdot \mathrm{e}^{r1 \cdot \frac{T-t+1}{T}} \cdot \sin(2\,\pi\, r1)\,. \quad (16)$$

The equation includes β as weight coefficient, *T* as the max number of iterations, and $r1$ as random number in [0, 1].

In the cyclone foraging strategy, individuals perform a random search with respect to the food as their reference position, which balances exploitation and exploration. To prioritize exploration, individuals can be forced to scan away from the current best position by randomly allocating a new position in the entire search space as a reference position. The mathematical equation for this mechanism is presented below:

$$x_{\text{rand}}^d = Lb^d + r \cdot (Ub^d - Lb^d), \quad (17)$$

$$x_i^d(t+1) = \begin{Bmatrix} x_{\text{rand}}^d + r \cdot \left(x_{\text{rand}}^d - x_i^d(t)\right) + \beta \cdot \left(x_{\text{rand}}^d - x_i^d(t)\right), i = 1 \\ x_{\text{rand}}^d + r \cdot \left(x_{i-1}^d(t) - x_i^d(t)\right) + \beta \cdot \left(x_{\text{rand}}^d - x_i^d(t)\right), i = 2..N \end{Bmatrix}. \quad (18)$$

The equation includes x_{rand}^d as a random position generated within the search space, and Ub^d and Lb^d as the upper and lower boundaries of the *d*-th dimension.

3.1.3. Somersault foraging

In somersault foraging, the food position is viewed as a pivot and individuals swim around it and somersault to a new position. This helps to update positions around the best solution found so far. The model is formulated as:

$$x_i^d(\mathrm{t}+1) = x_i^d(\mathrm{t}) + S \cdot \left(r_2 \cdot x_{\text{best}}^d - r_3 \cdot x_i^d(t)\right), i = 1..N, \quad (19)$$

The somersault range of manta rays is determined by the somersault factor, denoted as *S*, where *S* equals 2 multiplied by two random numbers (r_2 and r_3) between 0 and 1.

By updating their positions around the best solution found so far, individuals can move to any position in a new search domain. The range of somersault foraging reduces as iterations increase, allowing individuals to approximate gradually to the optimal solution.

3.2. dFDB algorithm

The dFDB technique is an evolved form of the FDB method, which was developed to offer more effective guidance in the search process [25]. Like the FDB method, the solution candidates in dFDB are chosen from the population based on their scores in a greedy manner. The score of a solution candidate is determined based on its fitness and range ratings. Therefore, the fitness ratings of applicants for the solution in a population P are indicated by the F-vector, as illustrated in (20). The distance range (DPi) necessary to evaluate the score of the ith solution candidate (Pi) can be derived using the Euclidean metric, which is defined in Equation (21). Here, P_i represents the *i*-th candidate and P_{best} represents the highest-ranking candidate in *P*.

$$F \equiv [f_1 \ldots\ldots f_n]^T, \quad (20)$$

$$D_{P_i} = \sqrt{(x_{1[i]} - x_{l[\text{best}]})^2 + \cdots .. + (x_{n[i]} - x_{n[\text{best}]})^2}\,. \quad (21)$$

The distance D_{P} that pertains to the P-population can be expressed in accordance with the equation provided as:

$$D_p \equiv [d_1 \ldots\ldots d_m]^T. \quad (22)$$

Prior to the computation of the scores of potential candidates' solution, the F vector outlined in Equation (20), and the distance vector (D_{p}) stipulated Equation (22) are subjected to normalization. The computation of the FDB score for the *i*-th solution candidate (SPi) is carried out using the following equation:

$$S_{P_i} = w \cdot normF_i + (1-w) \cdot normD_{P_i}, \quad (23)$$

The weighting coefficient w, which determines the impact of distance and fitness values on score calculation, is fixed at 0.5 in the FDB method. The solution candidates' FDB scores are expressed in Equation (24).

$$S_P \equiv [S_1 \ldots\ldots S_m]^T\,. \quad (24)$$

3.3. The proposed MRFO-*d*FDB

The MRFO-dFDB has two main components: foraging behaviour and dynamic fitness distance balance. The foraging behaviour component involves three steps: search, attack, and return. In the search phase, the rays explore the search space randomly. In the attack phase, they converge to the promising regions of the search space based on the prey density (the fitness value of the potential solutions). In the return phase, the rays return to the previously visited promising regions to avoid getting stuck in local optima.

The dynamic fitness distance balance component balances the exploitation and exploration of the search space. It involves dynamically adjusting the distance measure used to calculate the fitness value of the potential solutions. The distance measure is increased to encourage exploration and decreased to encourage exploitation. The pseudocode of the algorithm is given in Figure 3.

The algorithm starts with an initial population of rays, and it iteratively repeats the foraging behaviour and dynamic fitness distance balance components until the stopping criterion is met (maxFE). The best solution found by the algorithm is returned as the optimized solution.

The framework used to estimate the solar model parameters is depicted in Figure 4. First, the algorithm initializes the solar PV model, which serves as the basis for calculating the model

Pseudocode of the MRFO-*d*FDB Algorithm

Start

-*Initialize the population (solution candidates) Eq. (12).*

-*Use Eq.(11) and create the fitness vector Eq.(13).*

while *(search process up to maxFE)*

for i=1:N

If (rand<0.5) // *Cyclone foraging strategy*

If (t/Tmax<rand)

Xrand =X*i* +rand(X*ub*-X*i*)

calculate $x_i^d(t+1)$ using ***Eq. (18)***

End if

Else

calculate $x_i^d(t+1)$ using ***Eq. (15)***

End if

Else // (*d*FDB selection method)

$$x_i^d(t+1)=\begin{Bmatrix} x_i^d(t)+r.\left(x_{best}^d(t)-x_i^d(t)\right)+\alpha.\left(x_{dFDB}^d(t)-x_i^d(t)\right), i=1 \\ x_i^d(t)+r.\left(x_{i-1}^d(t)-x_i^d(t)\right)+\alpha.\left(x_{dFDB}^d(t)-x_i^d(t)\right), i=2..N \end{Bmatrix}$$

End if

// Updating Process

If (fitness of $x_i(t+1) > x_i(t)$ **then** $x_i(t) = x_i(t+1)$ and

If (fitness of $x_i(t) > x_{best}(t)$ **then** $x_{best}(t) = x_i(t)$

End if

End for

for i=1:N

$$x_i^d(t+1) = x_i^d(t) + S.(r_2.x_{best} - r_3.x_i(t))$$

End for

End while

Figure 3. MRFO-dFDB pseudocode.

parameters. Then, the algorithm reads the current and voltage measurements, which are used as inputs to the model. These measurements provide information on the performance of the solar PV system and are necessary for estimating the model parameters.

After that, the MRFO-dFDB takes over to localize the strongest candidate. This step involves minimizing Equation (12), which is the cost function used to evaluate the performance of the model. The goal of this step is to find the model parameters that best fit the current and voltage measurements. By minimizing the cost function, the algorithm can identify the strongest candidate among the potential solutions.

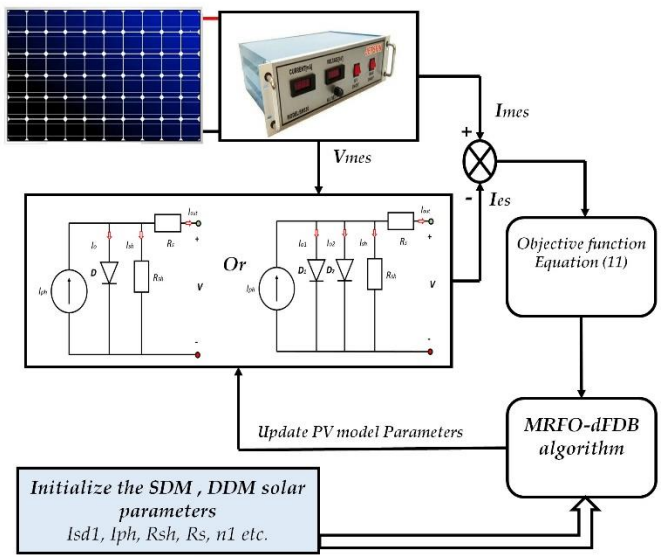

Figure 4. Proposed framework

Table 1. PV model.

PV type	Temp (◦C)	$N_s \times N_p$ Cells	PV model
STP6-120/36	55	36 × 1	SDM/DDM
Photowatt-PWP201	45	36 × 1	SDM/DDM

Table 2. MRFO-dFDB parameters.

Model	Population number (*P*)	Number of Iterations *maxFE*	number of decision variables (*dim*)
SDM	50	1000	1
DDM	50	1000	1

Table 3. Limits of the SDM and DDM model.

Parameter	STP6-120/36 Module		Photowatt-PWP201 Module	
	Ub	*Lb*	*Ub*	*Lb*
I_{sd1}, I_{sd2}	50	0	50	0
I_{ph}	8	0	2	0
R_s	0.36	0	2	0
R_{sh}	1500	0	2000	0
n_1, n_2	50	1	50	1

Table 4. Parameter extracted by MRFO-dFDB for SDM and DDM models.

PV type	PV model	I_{sd1}, I_{sd2} in µA	I_{ph} in A	R_s in Ω	R_{sh} in Ω	n_1, n_2
STP6	SDM	2.27, -	7.4553	0.0046	950.303	1.257, -
	DDM	10.8, 2.375	7.457	0.00459	213.353	31.8, 1.3521
PWP201	SDM	4.59, -	1.026	0.0329	69.5824	1.38, -
	DDM	1.98,1.581	1.0328	0.0352	18.8596	1.344, 13.81

Finally, the MRFO-dFDB outputs the best solution, which is the set of model parameters that minimize the cost function. This set of parameters represents the best fit between the model and the measured data, and can be used to improve the performance of the solar PV system.

4. IMPLEMENTATION SETUP

The suggested MRFO-dFDB algorithm (Figure 4) is applied to evaluate the parameters of solar PV models using STP6-120/36 and PWP201 PV modules [26] (both for DDM and SDM model) and compared with WOS (War Strategy Optimization Algorithm) [27] and SFO (Sunflower Optimization Algorithm) [28]. The STP6-120/36 module is monocrystalline and the PWP201 module is polycrystalline (see Table 1), both having 36 cells in series. In order to derive the solar PV model parameters, the MRFO-dFDB algorithm settings are defined Table 2 and Table 3.

5. RESULTS AND DISCUSSION

5.1. SDM results

The main target is to retrieve the parameters: I_{sd}, I_{ph}, R_{sh}, R_s, and n for the SDM PV modules STP6-120/36 and Photowatt-PWP201. Table 3 presents the lower and upper boundaries of these parameters. The *P-V* and *I-V* characteristics of the modules using MRFO-dFDB, WOS, and SFO are plotted in Figure 6. The loss function convergence curves are shown in Figure 7 and Figure 8, and the absolute current error is shown in Figure 9 and Figure 10 respectively. The parameters extracted by MRFO-dFDB are enumerated in Table 4 (for all tests SDM and DDM).

5.2. DDM results

Considering the DDM, a total of 7 parameters, which include I_{sd2}, I_{sd1}, I_{ph}, R_{sh}, R_s, n_1, n_2, needs to be retrieved. The upper and lower boundaries for these metrics can be found in Table 3.

Figure 11 and Figure 12 indicate the I-V and P-V features of the PV using MRFO-dFDB, WOS and SFO. The loss function convergence curves are displayed in Figure 13 and Figure 14, while Figure 15 and Figure 16 show the absolute current error plot. The retrieved parameters by MRFO-dFDB are reported in Table 4.

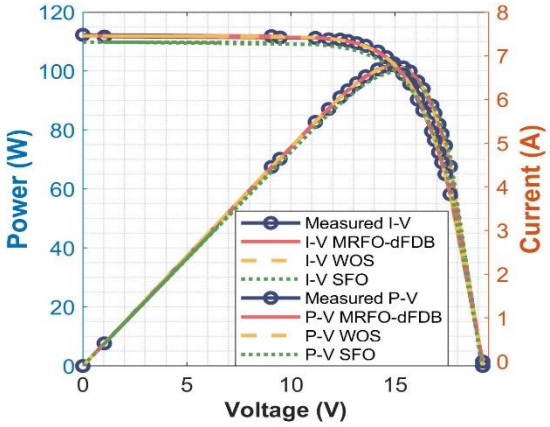

Figure 5. I-V and P-V curves for SDM model (STP6 module).

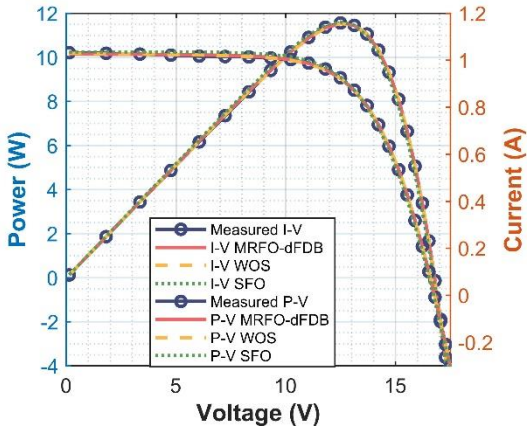

Figure 6. I-V and P-V curves for SDM model (PWP201 module)

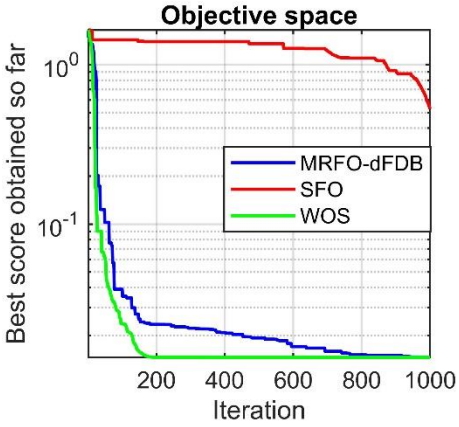

Figure 7. Convergence curve SDM (STP6 module)

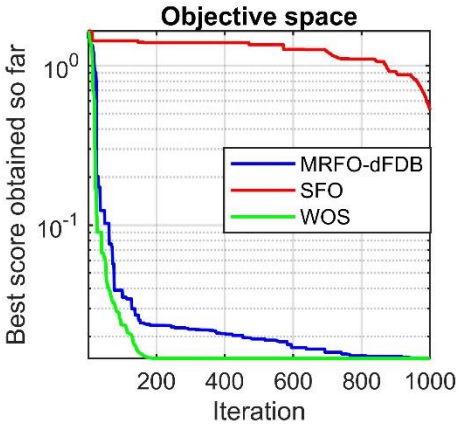

Figure 8. Convergence curve SDM (PWP201 module).

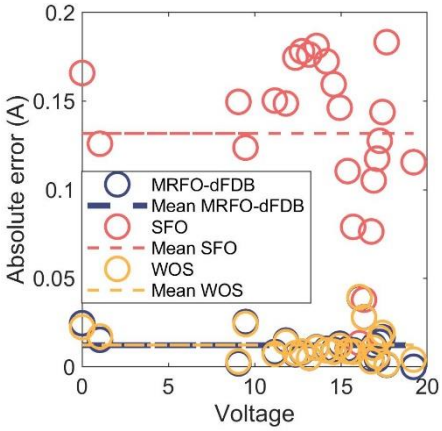

Figure 9. Absolute current and mean errors in SDM model (STP6)

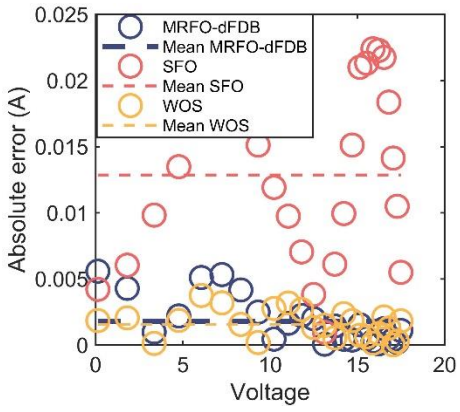

Figure 10. Absolute current and mean errors in SDM model (PWP201)

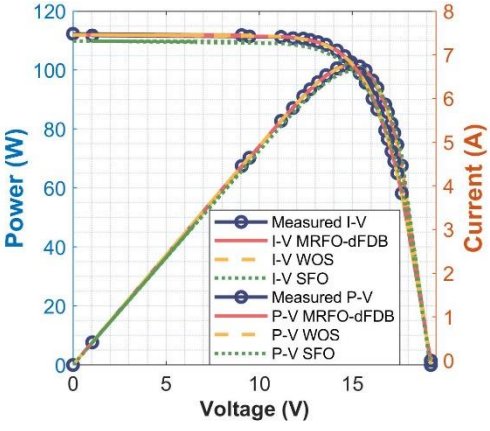

Figure 11. I-V and P-V curves for DDM model (STP6 module).

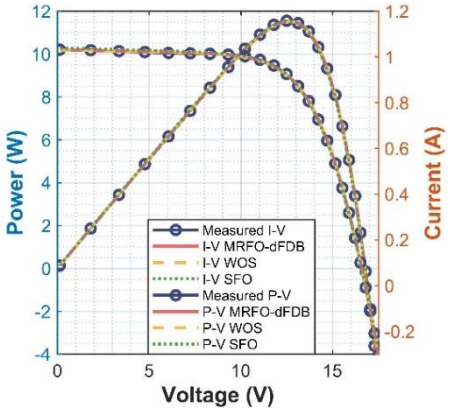

Figure 12. I-V and P-V curves for DDM model (PWP201 module)

5.3. Discussion

To gauge the validity of the approaches, we evaluate their predictive efficiency by means of three measures: mean square error (MSE), root mean square error (RMSE), normalized RMSE (NRMSE) denoted by:

$$MSE = \frac{1}{m}\sum_{k=1}^{m}(I_{\mathrm{es}}(k) - I_{\mathrm{tr}}(k))^2\,, \tag{25}$$

$$NRMSE = \frac{RMSE}{I_{\mathrm{es,max}} - I_{\mathrm{es,min}}}, \tag{26}$$

$$RMSE = \sqrt{\frac{1}{m}\sum_{k=1}^{m}[(I_{\mathrm{es}}(k) - I_{\mathrm{tr}}(k)]^2}\,, \tag{27}$$

where m equals the number of points, I_{es} and I_{tr} represent the measured and estimated output current.

Table 5 summarizes the different calculated indicators of the methods applied to identify PV solar parameters for the STP6-120/36 and Photowatt-PWP201modules. The MSE, RMSE, and NRMSE are employed to assess the algorithms' performance.

From the results: For SDM, we can observe that MRFO-dFDB and WOS show similar performance with RMSE values of 15.2 in STP6 and 2.4, and 1.87 mA for PWP201 respectively. In addition, the NRMSE values are slightly close apart from the STP6 case where WOS is slightly better. The SFO approach clearly underperforms, with RMSE values of 138.9 and 14.33 mA and a high NRMSE value of 0.0186 and 0.0107.

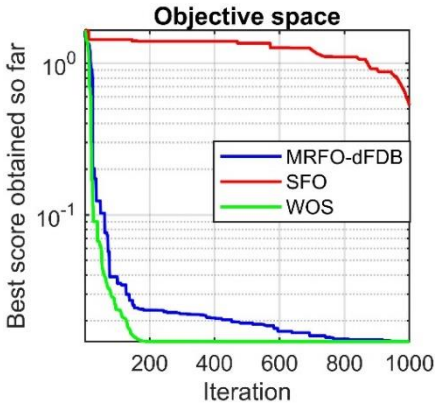

Figure 13. Convergence curve DDM (STP6 module)

Table 5. Predictive performance indicators for STM for SDM and DDM.

PV type	PV model	Methods	*RMSE* in mA	*NRMSE*	*MSE*
STP6	SDM	MRFO-dFDB	15.2	0.0020	2.3e-4
		WOS	15.2	0.0020	2.2e-4
		SFO	138.9	0.0186	0.0193
	DDM	MRFO-dFDB	15.3	0.0020	2.3e-4
		WOS	15.2	0.0020	2.29e-4
		SFO	135.2	0.0184	0.019
PWP201	SDM	MRFO-dFDB	2.4	0.0018	6.15e-6
		WOS	1.87	0.0014	3.5e-6
		SFO	14.33	0.0107	2.05e-4
	DDM	MRFO-dFDB	1.91	0.0014	3.67e-6
		WOS	1.87	0.0014	3.52e-6
		SFO	77.88	0.0046	3.48e-05

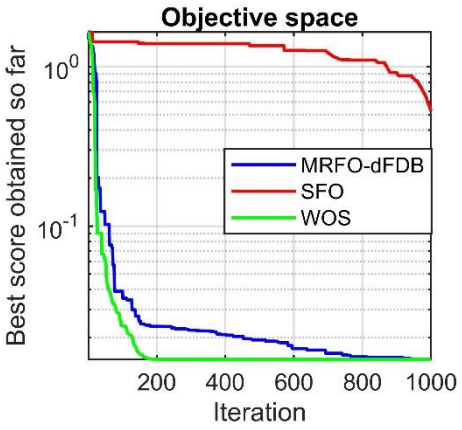

Figure 14. Convergence curve DDM (PWP201 module).

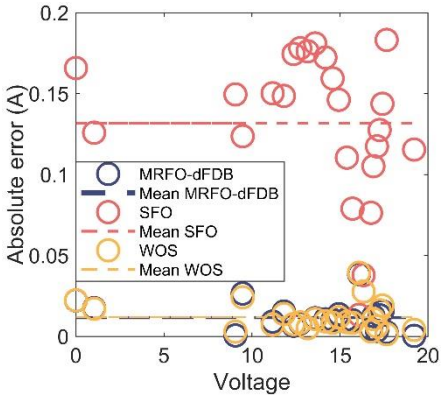

Figure 15. Absolute current and mean errors in DDM model (STP6).

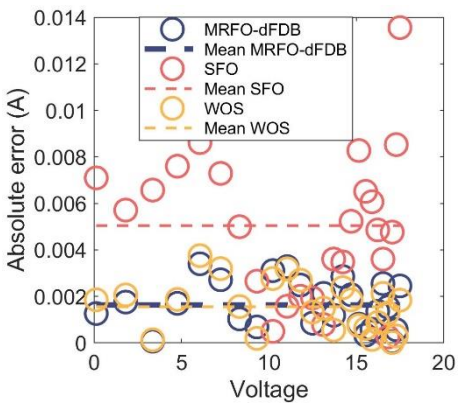

Figure 16. Absolute current and mean errors in DDM model (PWP201).

Similar to SDM, the MRFO-dFDB and WOS showed close results with WOS being slightly better. The SFO algorithm has high values for RMSE and NRMSE.

MSE reflects the closeness of the predicted values to the measured values.

When examining the MSE values, we are able to note that: MRFO-dFDB and WOS have the smallest MSE values for the SDM and DDM cases (WOS being slightly better), suggesting that both methods are capable of providing precise predictions. In the SDM case, the MSE value for MRFO-dFDB is 2.3 10^{-4} and 6.15 10^{-6}, while WOS recorded 2.2 10^{-4} and 3.5 10^{-6}, while in the MDD, MRFO-dFDB recorded 2.3 10^{-4} and 3.67 10^{-6}, which is quite close to WOS that recorded 2.29 10^{-4} and 3.52 10^{-6}.

The SFO shows the largest MSE values amongst the three methodologies for the SDM and DDM cases. In the SDM case, the MSE value for SFO is 0.0193 and 2.05 10^{-4}, while in the DDM case, the MSE values are 0.019 and 3.48 10^{-5}.

Table 6 summarizes the max, mean, min, and power errors (Equation (28)) for the different algorithms.

$$P_{\text{error}} = \frac{1}{m}\sum_{i=1}^{m} |P_{\text{est}}(i) - P_{\text{meas}}(i)|\,, \tag{28}$$

where P_{est} and P_{meas} are the estimated and measured power, and m being the number of points.

When looking at the algorithms' performance, the MRFO-dFDB algorithm shows the greatest performance over all, with the lowest maximum error in all tests, except for the SDM (STP6) case. The WOS algorithm's performance is fairly comparable to that of the MRFO-dFDB algorithm, with significantly higher maximum error values. In contrast, SFO algorithm underperforms substantially, having the worst peak and power error values and fairly high average error values.

The same conclusion can be drawn for the power error, we can see that the MRFO-dFDB algorithm performs better than the other algorithms, except for the DDM (PWP201) case.

Moreover, the performance of MRFO-dFDB is evaluated against the WOS and SFO in terms of computational speed. We used MATLAB software on an Asus laptop with an Intel Core i7 processor running at 2.6 GHz and 8 GB of memory. We executed the individual algorithms and measured the running time for 1000 iterations, results are collected in Table 7.

As can be seen, the WOS method takes more time to estimate the PV model parameters, over 100 seconds in all tests.

Table 6. Absolute Max, Min, Mean, and power error of the algorithms.

PV type	PV model	Methods	Max error in mA	Min error in mA	Mean error in mA	Power error in mW
STP6	SDM	MRFO-dFDB	39.02	0.044	12.26	155.42
		WOS	39.38	1.443	12.34	158.24
		SFO	183.3	13.41	131.8	171.9
	DDM	MRFO-dFDB	38.61	0.422	12.413	157.63
		WOS	39.38	1.443	12.34	158.24
		SFO	153.3	10.41	130	165.9
PWP201	SDM	MRFO-dFDB	5.33	0.068	1.790	14.122
		WOS	3.752	0.015	1.551	16.211
		SFO	22.40	0.964	12.861	159.56
	DDM	MRFO-dFDB	3.40	0.041	1.631	18.390
		WOS	3.75	0.014	1.55	16.211
		SFO	13.56	0.252	5.042	174.50

Table 7. Computation speed in seconds.

PV type	PV model	MRFO-dFDB	WOS	SFO
STP6	SDM	20.779	100.946	22.122
	DDM	30.10	114.120	24.347
PWP201	SDM	21.43	162.872	24.201
	DDM	23.50	174.50	25.50

On the other hand, SFO is the second fastest, however, their accuracy is low (Table 5 and Table 6). SFO scored the highest errors. Moreover, their indicators (RMSE, NRMSE, MSE) are higher than those of WOS and MRFO-dFDB.

MRFO-dFDB being close in performance to WOS is the fastest except DDM (STP6). We can state that MRFO-dFDB has a fair trade-off between precision and rapidity.

Altogether, the results in the tables give a useful summary of the performance of the different algorithms in solar PV parameter estimation. The results imply that MRFO-dFDB is a very promising approach to achieve solar PV parameter estimation.

6. CONCLUSION

In conclusion, the MRFO-dFDB algorithm emerges as an efficient approach for accurately estimating solar PV model parameters. Through the integration of fitness distance balance, the algorithm effectively balances exploration and exploitation, facilitating the rapid identification of optimal parameters while adapting to changes within the search space.

Applying MRFO-dFDB to extract parameters from the STP6-120/36 and Photowatt-PWP201 solar modules yields exceptional predictive performance for both single diode (SDM) and double diode (DDM) models. In comparison to state-of-the-art methods such as SFO and WOS, MRFO-dFDB outperforms them. While achieving comparable predictive performance to WOS, MRFO-dFDB stands out with significantly faster computation speed. Moreover, MRFO-dFDB surpasses SFO in terms of RMSE, NRMSE, and MSE values, indicating its superior accuracy.

Specifically, MRFO-dFDB achieves lower RMSE values, namely less than 15.3 mA for the STP6-120/36 module and less than 2.4 mA for the Photowatt-PWP201 module. Additionally, it demonstrates lower maximum errors of 39.02 mA and 5.33 mA, as well as lower power errors of 155.42 mW and 14.122 mW, for the STP6-120/36 and Photowatt-PWP201 solar modules, respectively. Furthermore, it exhibits excellent performance with faster computation speed, taking less than 30.1 seconds in all tests, further highlighting its superiority.

Overall, the results affirm the potential of MRFO-dFDB in accurately estimating solar PV system parameters, while offering enhanced computational efficiency. These findings underscore its value in optimizing PV system design and performance.

REFERENCES

[1] S. I. Selem, H. M. Hasanien, A. A. El-Fergany, Parameters extraction of PEMFC's model using manta rays foraging optimizer, International Journal of Energy Research 4(6) (2020), pp. 4629-4640.
DOI: 10.1002/er.5244

[2] M. Wang, X. Zhao, A. A. Heidari, H. Chen, Evaluation of constraint in photovoltaic models by exploiting an enhanced ant lion optimizer, Solar Energy 211 (2020), pp. 503-521.
DOI: 10.1016/j.solener.2020.09.080

[3] X. Chen, H. Tianfield, C. Mei, W. Du, G. Liu, Biogeography-based learning particle swarm optimization, Soft Computing 21 (2017), pp. 7519-7541.
DOI: 10.1007/s00500-016-2307-7

[4] G. Xiong, J. Zhang, D. Shi, L. Zhu, X. Yuan, Z. Tan, Winner-leading competitive swarm optimizer with dynamic Gaussian mutation for parameter extraction of solar photovoltaic models, Energy Conversion and Management 206 (2020), art. No. 112450.
DOI: 10.1016/j.enconman.2019.112450

[5] E. I. Batzelis, S. A. Papathanassiou, A method for the analytical extraction of the single-diode PV model parameters, IEEE Transactions on Sustainable Energy 7(2) (2015), pp. 504-512.
DOI: 10.1109/TSTE.2015.2503435

[6] P. Changmai, S. K. Nayak, S. K. Metya, Estimation of PV module parameters from the manufacturer's datasheet for MPP estimation, IET Renewable Power Generation 14(11) (2020), pp. 1988-1996.
DOI: 10.1049/iet-rpg.2019.1377

[7] Y.-C. Huang, C.-M. Huang, S.-J. Chen, S.-P. Yang, Optimization of module parameters for PV power estimation using a hybrid algorithm, IEEE Transactions on Sustainable Energy 11(4) (2019), pp. 2210-2219.
DOI: 10.1109/TSTE.2019.2952444

[8] D. H. Muhsen, A. B. Ghazali, T. Khatib, I. A. Abed, Parameters extraction of double diode photovoltaic module's model based on hybrid evolutionary algorithm, Energy Conversion and Management 105 (2015), pp. 552-561.
DOI: 10.1016/j.enconman.2015.08.023

[9] S. Gao, K. Wang, S. Tao, T. Jin, H. Dai, J. Cheng, A state-of-the-art differential evolution algorithm for parameter estimation of solar photovoltaic models, Energy Conversion and Management 230 (2021), art. No. 113784.
DOI: 10.1016/j.enconman.2020.113784

[10] D. Saadaoui, M. Elyaqouti, K. Assalaou, S. Lidaighbi, Parameters optimization of solar PV cell/module using genetic algorithm based on non-uniform mutation, Energy Conversion and Management: X 12 (2021), art. No. 100129.
DOI: 10.1016/j.ecmx.2021.100129

[11] C. Touabi, A. Ouadi, H. Bentarzi, Photovoltaic panel parameters estimation using an opposition based initialization particle swarm Optimization, Engineering Proceedings 29(1) (2023).
DOI: 10.3390/engproc2023029016

[12] Shuijia Li, Wenyin Gong, Xuesong Yan, Chengyu Hu, Danyu Bai, Ling Wang, Liang Gao, Parameter extraction of photovoltaic models using an improved teaching-learning-based optimization, Energy Conversion and Management 186 (2019), pp. 293-305.
DOI: 10.1016/j.enconman.2019.02.048

[13] Mingzhang Pan, Chao Li, Ran Gao, Yuting Huang, Hui You, Tangsheng Gu, Fengren Qin, Photovoltaic power forecasting based on a support vector machine with improved ant colony optimization, Journal of Cleaner Production 277 (2020), art. No. 123948.
DOI: 10.1016/j.jclepro.2020.123948

[14] M. Premkumar, P. Jangir, R. Sowmya, R. M. Elavarasan, B. S. Kumar, Enhanced chaotic JAYA algorithm for parameter estimation of photovoltaic cell/modules, ISA transactions 116 (2021), pp. 139-166.
DOI: 10.1016/j.isatra.2021.01.045

[15] G. Xiong, J. Zhang, D. Shi, X. Yuan, Application of supply-demand-based optimization for parameter extraction of solar photovoltaic models, Complexity 2019 (2019), pp. 1-22.
DOI: 10.1155/2019/3923691

[16] G. Xiong, J. Zhang, X. Yuan, D. Shi, Y. He, Application of symbiotic organisms search algorithm for parameter extraction of solar cell models, Applied Sciences 8(11) (2018), art. No. 2155.
DOI: 10.3390/app8112155

[17] A. Fathy, H. Rezk, Parameter estimation of photovoltaic system using imperialist competitive algorithm, Renewable Energy 11 (2017), pp. 307-320.
DOI: 10.1016/j.renene.2017.04.014

[18] D. Alam, D. Yousri, M. Eteiba, Flower pollination algorithm based solar PV parameter estimation, Energy Conversion and Management 101 (2015), pp. 410-422.
DOI: 10.1016/j.enconman.2015.05.074

[19] W. Long, J. Jiao, X. Liang, M. Xu, M. Tang, S. Cai, Parameters estimation of photovoltaic models using a novel hybrid seagull optimization algorithm, Energy 249 (2022), art. No. 123760.
DOI: 10.1016/j.energy.2022.123760

[20] A. Singh, A. Sharma, S. Rajput, A. Bose, X. Hu, An investigation on hybrid particle swarm optimization algorithms for parameter optimization of PV cells, Electronics 11(6) (2022), art. No. 909.
DOI: 10.3390/electronics11060909

[21] M. Eslami, E. Akbari, S. T. Seyed Sadr, B. F. Ibrahim, A novel hybrid algorithm based on rat swarm optimization and pattern search for parameter extraction of solar photovoltaic models, Energy Science & Engineering 10(8) (2022), pp. 2689-2713.
DOI: 10.1002/ese3.1160

[22] R. B. Messaoud, Extraction of uncertain parameters of double-diode model of a photovoltaic panel using Ant Lion Optimization, SN Applied Sciences 2(2) (2020), art. no. 239.
DOI: 10.1007/s42452-020-2013-z

[23] M. Abdel-Basset, R. Mohamed, R. K. Chakrabortty, K. Sallam, M. J. Ryan, An efficient teaching-learning-based optimization algorithm for parameters identification of photovoltaic models: Analysis and validations, Energy Conversion and Management 227 (2021), art. No. 113614.
DOI: 10.1016/j.enconman.2020.113614

[24] W. Zhao, Z. Zhang, L. Wang, Manta ray foraging optimization: An effective bio-inspired optimizer for engineering applications, Engineering Applications of Artificial Intelligence 87 (2020), art. No. 103300.
DOI: 10.1016/j.engappai.2019.103300

[25] H. T. Kahraman, H. Bakir, S. Duman, M. Katı, S. Aras, U. Guvenc, Dynamic FDB selection method and its application: modeling and optimizing of directional overcurrent relays coordination, Applied Intelligence (2022), pp. 1-36.
DOI: 10.1007/s10489-021-02629-3

[26] S. Li, W. Gong, X. Yan, C. Hu, D. Bai, L. Wang, Parameter estimation of photovoltaic models with memetic adaptive differential evolution, Solar Energy 190 (2019) pp. 465-474.
DOI: 10.1016/j.solener.2019.08.022

[27] T. S. Ayyarao, P. P. Kumar, Parameter estimation of solar PV models with a new proposed war strategy optimization algorithm, International Journal of Energy Research 47(6) (2022), pp. 7215-7238.
DOI: 10.1002/er.7629

[28] M. H. Qais, H. M. Hasanien, S. Alghuwainem, Identification of electrical parameters for three-diode photovoltaic model using analytical and sunflower optimization algorithm, Applied Energy 250 (2019), pp. 109-117.
DOI: 10.1016/j.apenergy.2019.05.013